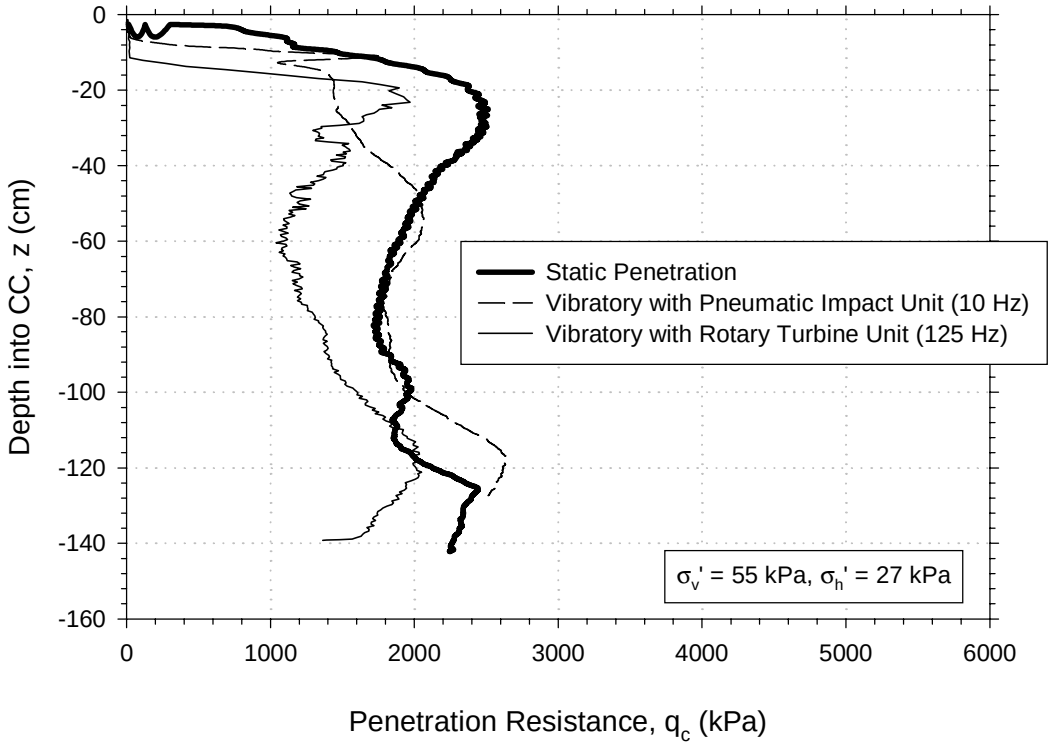

Figure 6.1 Influence of Vibration on Penetration Resistance Using Different Vibratory Units

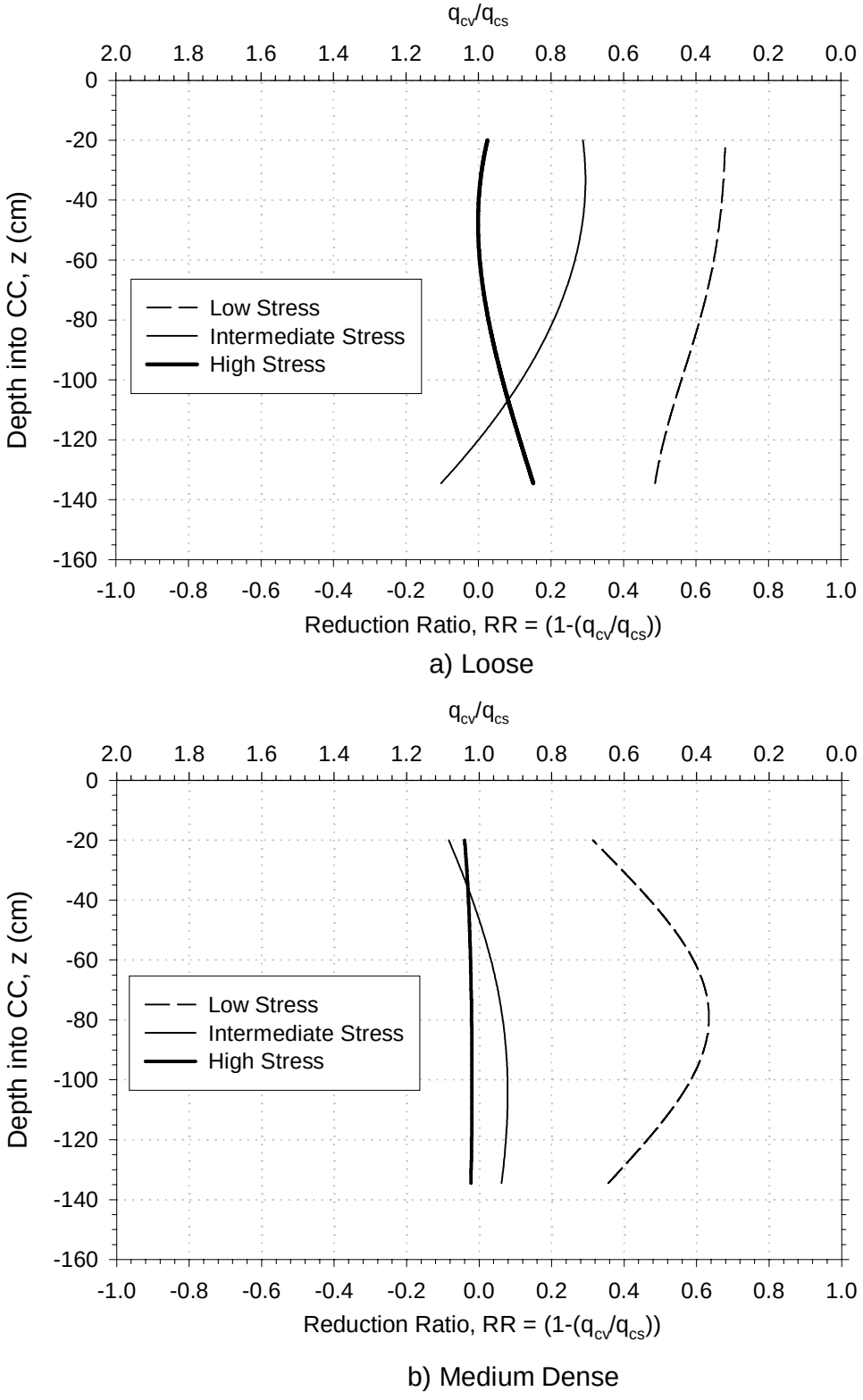

Figure 6.2 Reduction Ratio versus Depth for Different Density and Stress Levels

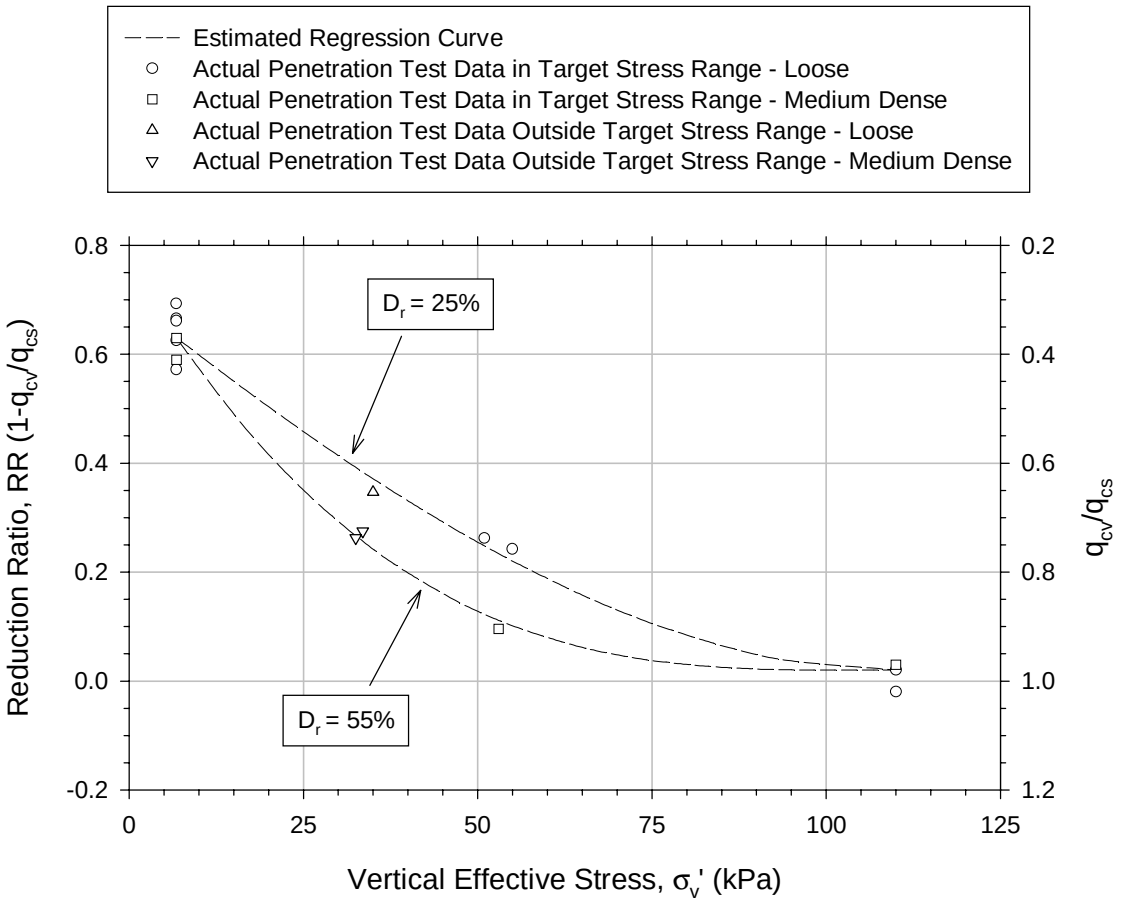

Figure 6.3 Comparison of Reduction Ratios Measured through Calibration Chamber Testing to that Estimated Using a Regression Analysis

$$RR = [C_1 \cdot D_r][C_2 + \sigma_v']^2[C_3 + \sigma_v'] + C_4[C_5 + \sigma_v'] \cdot [C_6 + (C_7 + \sigma_v') \cdot \sigma_v']$$

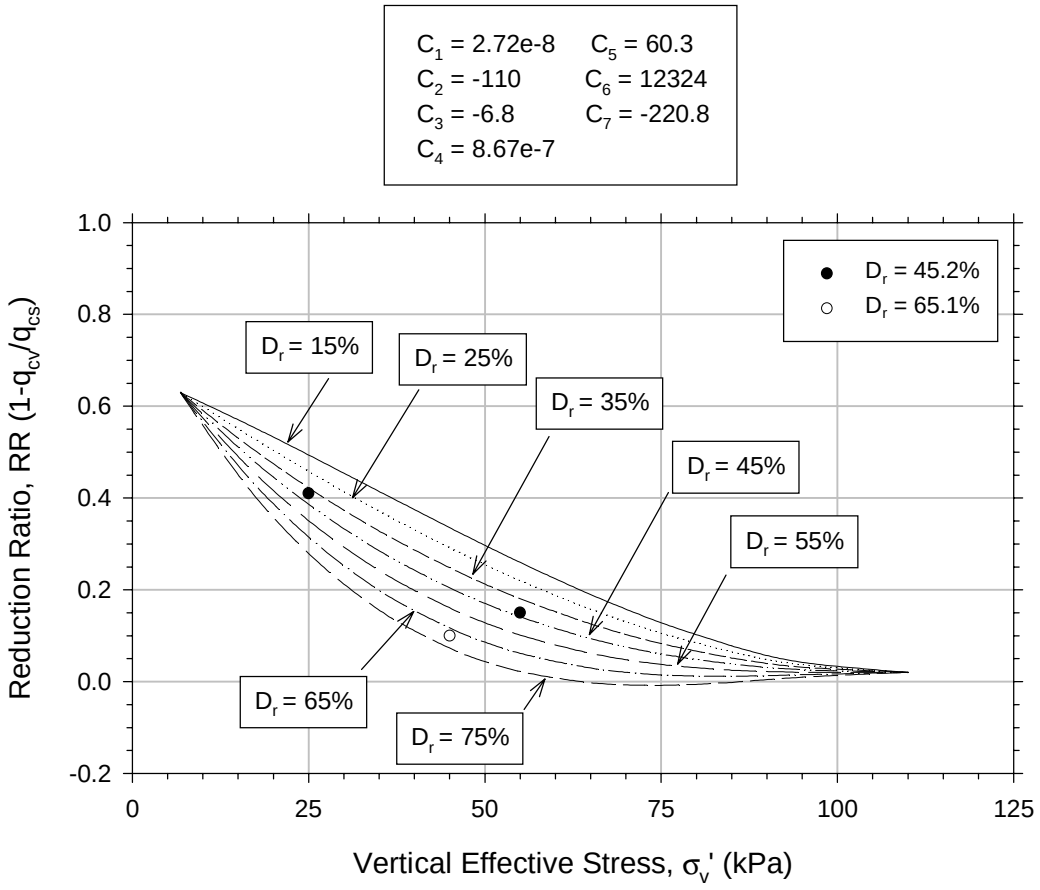

Figure 6.4 Family of Curves Generated From Empirical Correlations

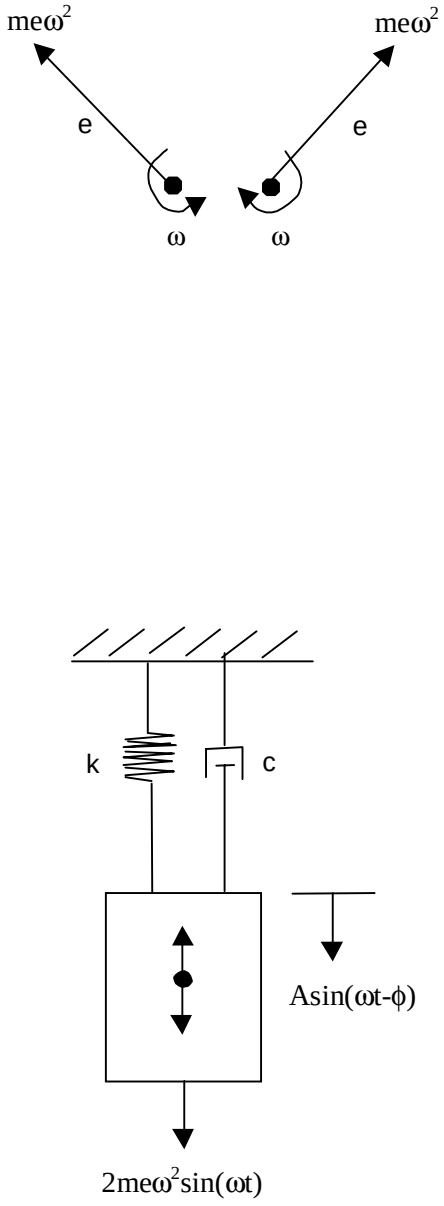

Figure 6.5 Mechanics of Counter Rotating Mass Vibration System

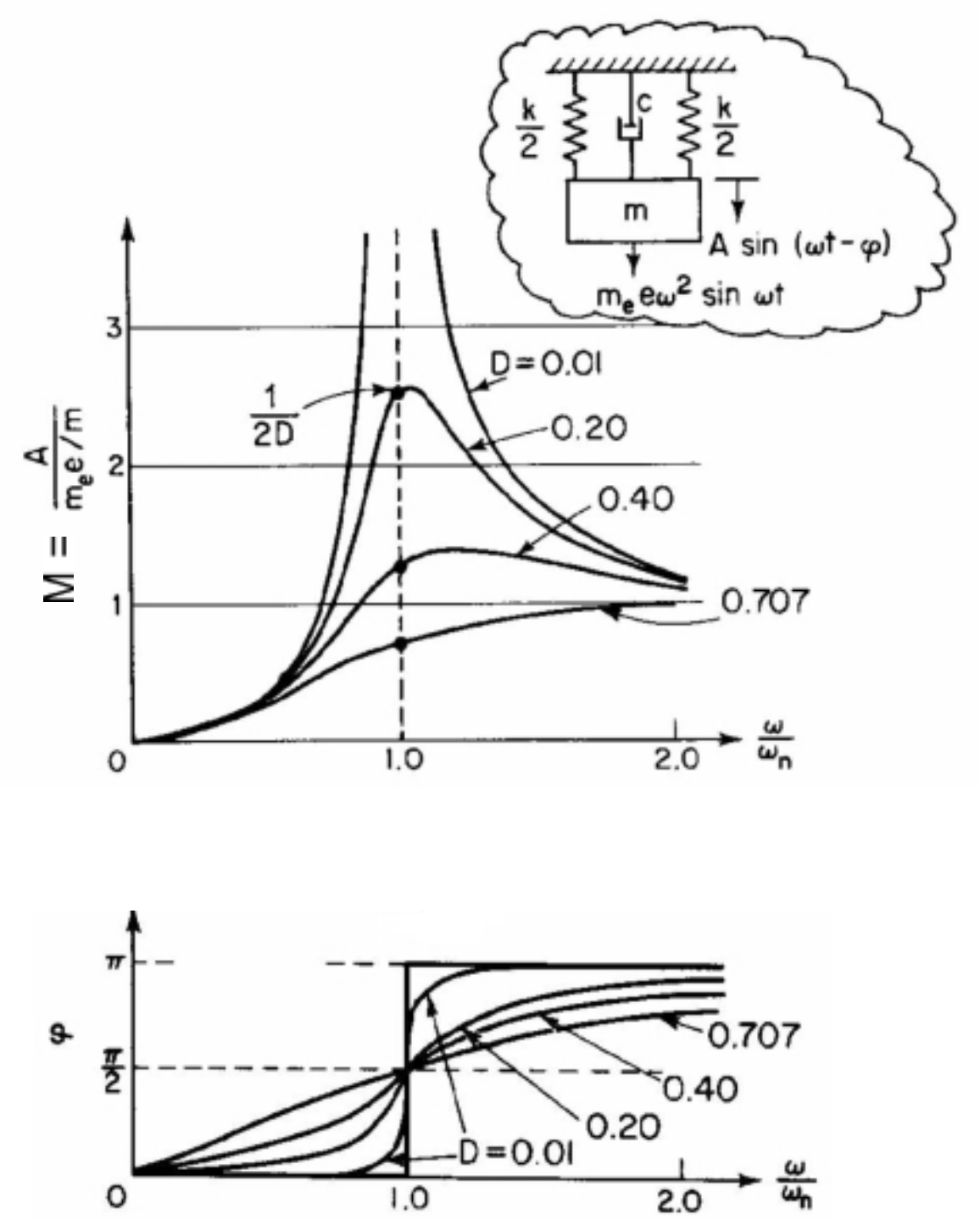

Figure 6.6 Response Curves for Rotating Mass Type Excitation of a Viscously Damped Single Degree of Freedom System (After Richart et al. 1970)

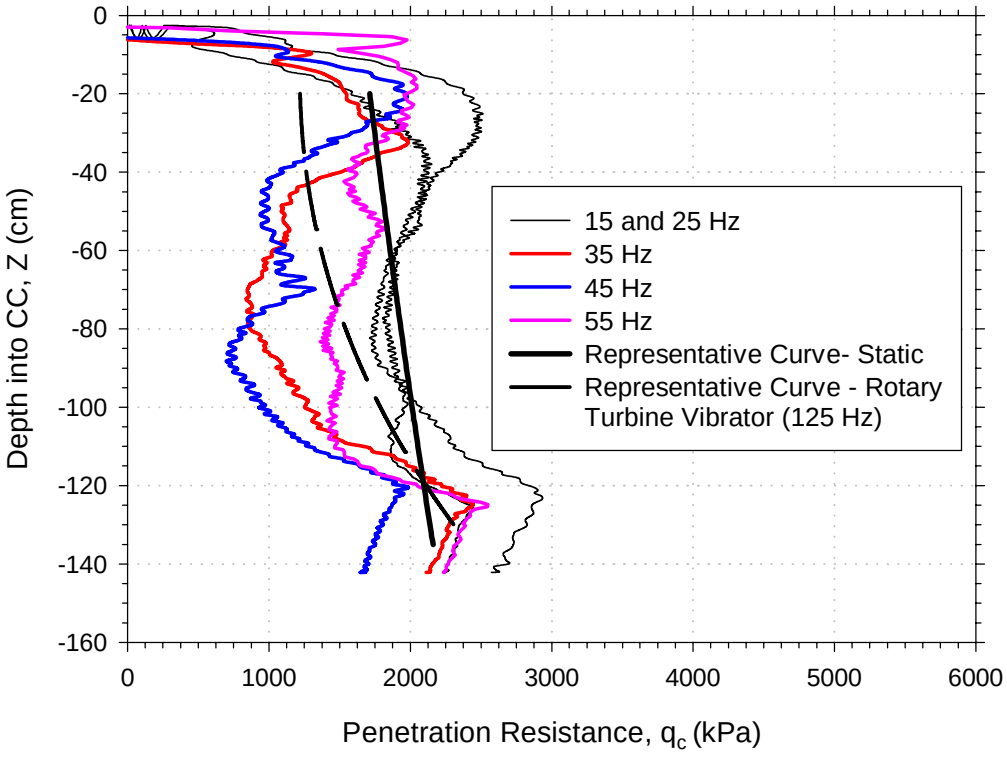

a) Loose

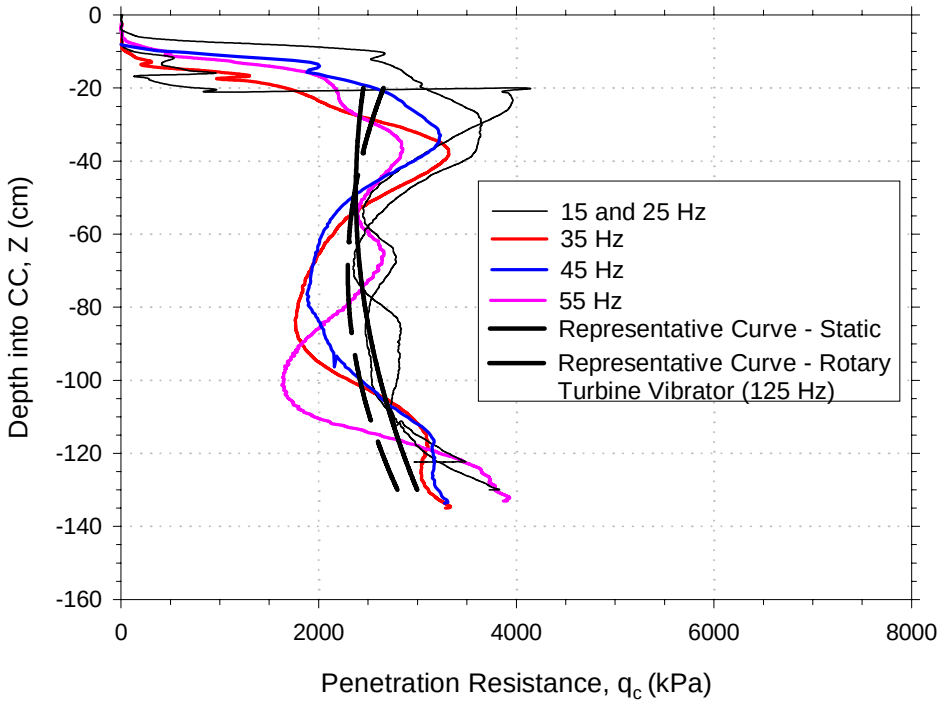

b) Medium Dense

Figure 6.7 Effects of Vibration Frequency on Penetration Resistance Value at Intermediate Stress Levels

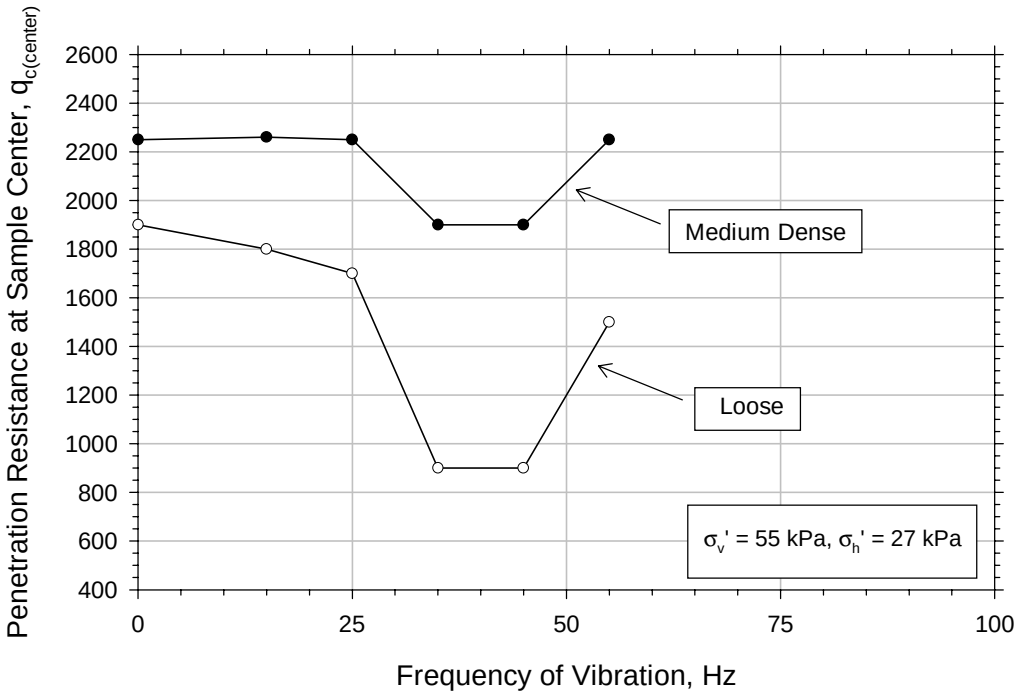

Figure 6.8 Influence of Vibration Frequency on Penetration Resistance Value for Different Density Soils Using the Counter Rotating Mass Vibrator

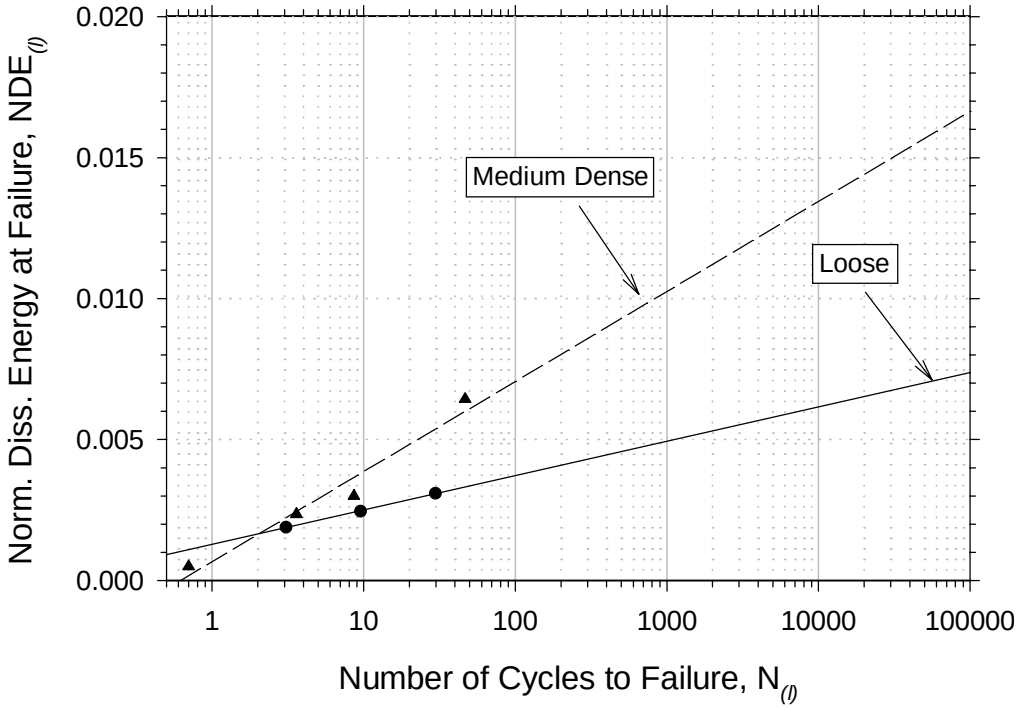

a) NDE from Cyclic Triaxial Tests

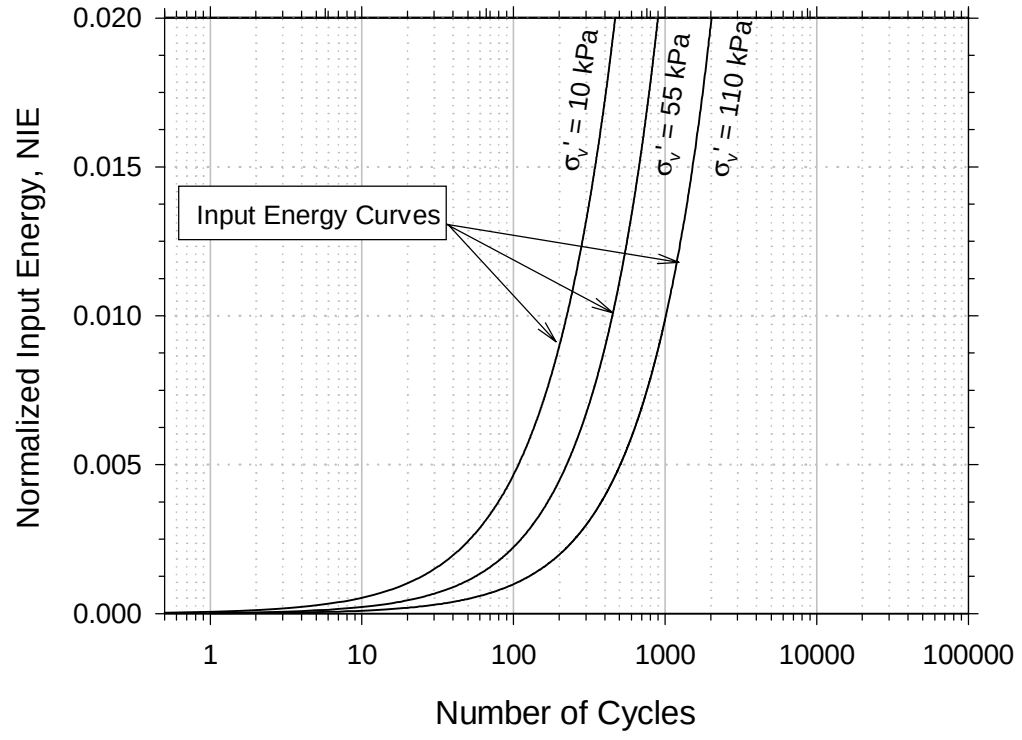

b) NIE from Vibrator

Figure 6.9 NDE and NIE Plots generated from Triaxial Test Data and Vibration

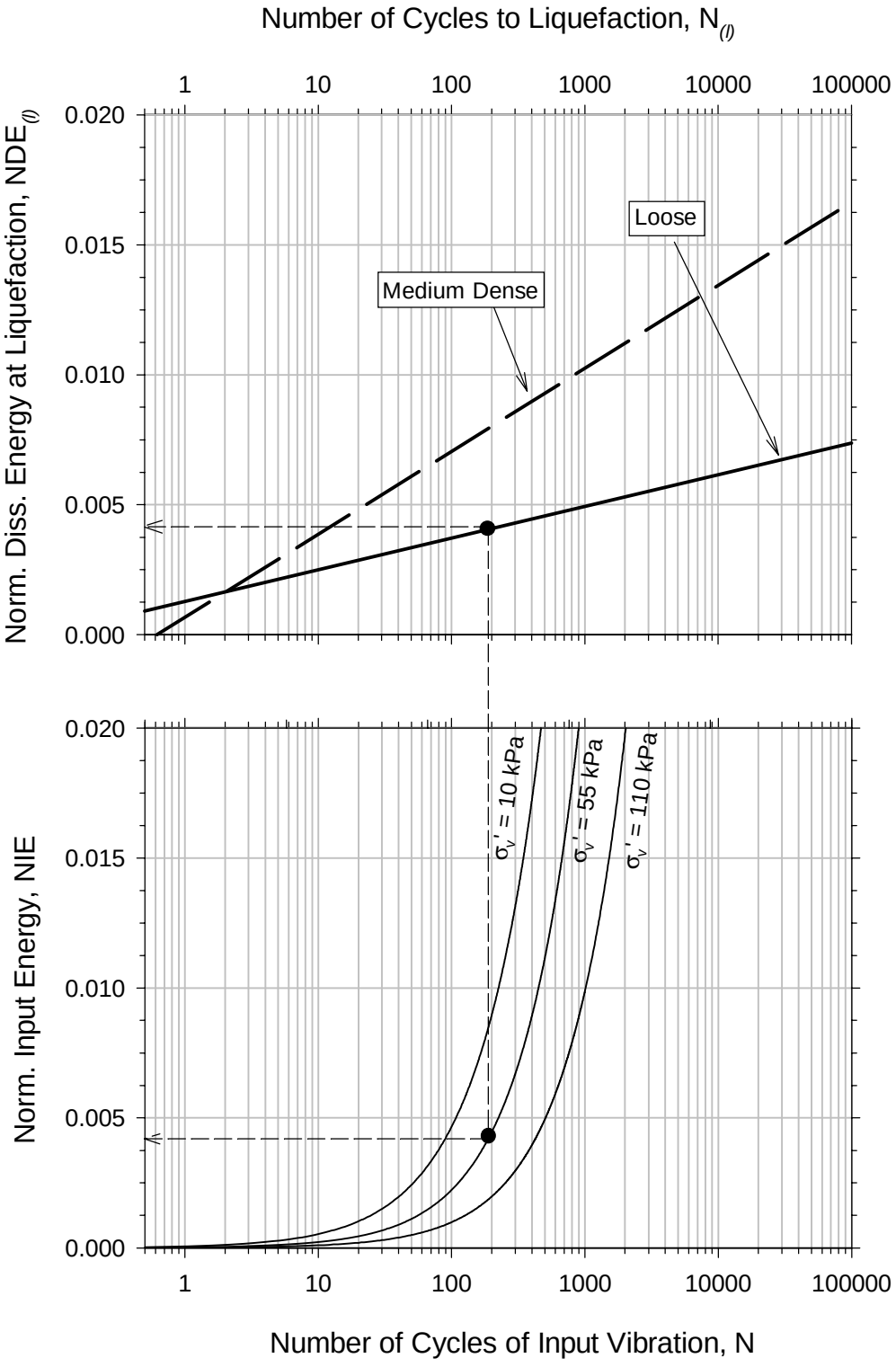

Figure 6.10 Example of Procedure Used to Determine Number of Cycles Needed to Cause Soil Strength Loss Within Zone of Influence of Cone Penetrometer

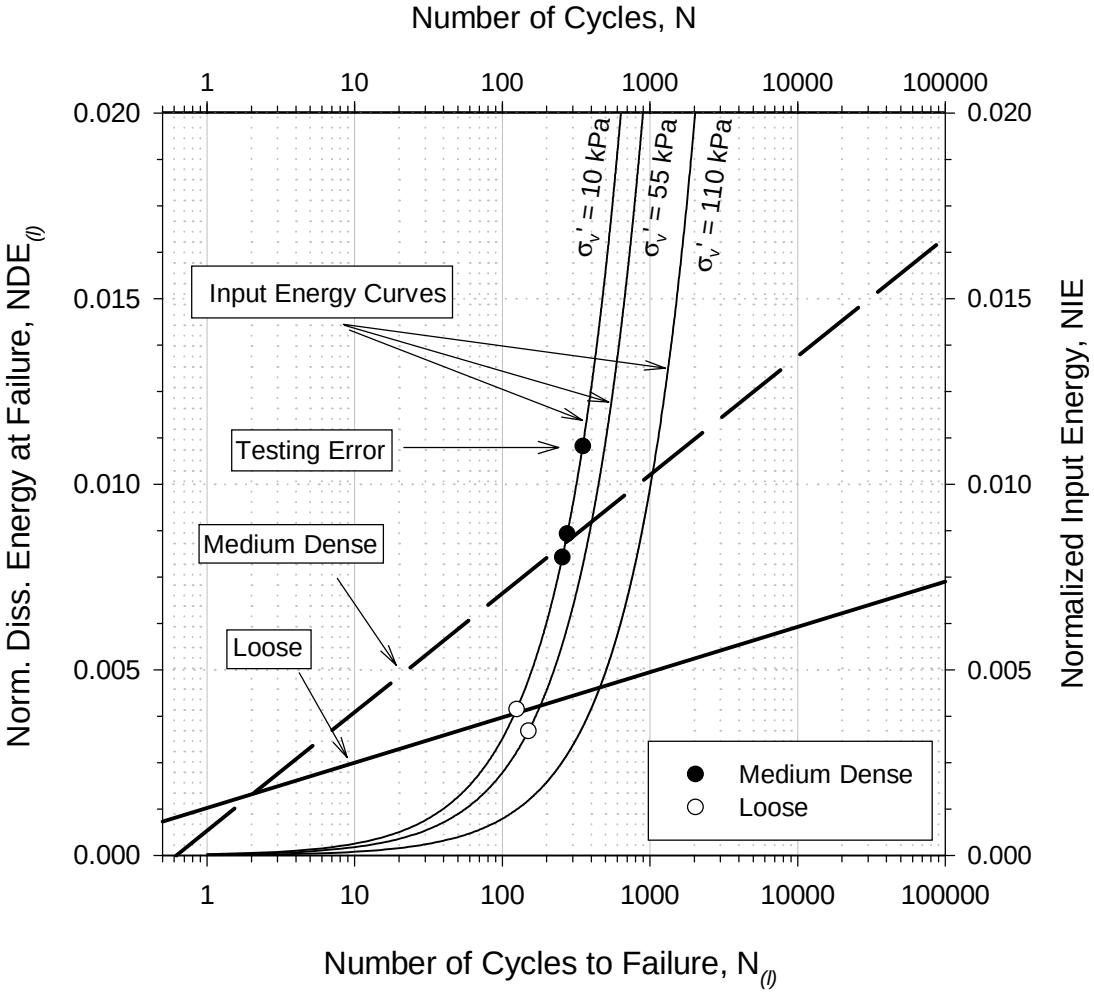

Figure 6.11 Comparison of Test Data to Estimated Condition of Soil Strength Loss